Available online at www.sciencedirect.com
SCIENCE DIRECT
Polymer 46 (2005) 9362–9377
polymer
www.elsevier.com/locate/polymer

Solvent-induced microdomain orientation in polystyrene-*b*-poly(L-lactide) diblock copolymer thin films for nanopatterning

Rong-Ming Ho[a,b,*], Wen-Hsien Tseng[a], Hui-Wen Fan[c], Yeo-Wan Chiang[a], Chu-Chieh Lin[d], Bao-Tsan Ko[b], Bor-Han Huang[d]

[a]*Department of Chemical Engineering, National Tsing-Hua University, Hsinchu 30013, Taiwan, ROC*
[b]*Union Chemical Laboratories, Industrial Technology Research Institute, Hsinchu 30013, Taiwan, ROC*
[c]*Department of Chemical Engineering, National Chung-Hsing University, Taichung 40227, Taiwan, ROC*
[d]*Department of Chemistry, National Chung-Hsing University, Taichung 40227, Taiwan, ROC*

Received 15 April 2005; received in revised form 7 July 2005; accepted 8 July 2005
Available online 15 August 2005

Abstract

A series of degradable block copolymers, polystyrene-*b*-poly(L-lactide) (PS–PLLA), with PLLA hexagonal cylinder (HC) morphology has been synthesized in this study. Well-oriented, perpendicular PLLA cylinders of PS–PLLA thin films were efficiently achieved by spin coating using appropriate solvents regardless of the use of substrates. After hydrolysis of PLLA, well-oriented HC nanochannel arrays over large area in addition to uniform surface with controlled thickness and domain size were obtained; providing a simple and efficient path to prepare nanopatterned templates for applications. The induced orientation of PS–PLLA microdomains was strongly dependent upon the evaporation rate of solvent and its solubility between constituted blocks. The origins for the formed perpendicular HC morphology were systematically studied. The primary concern of controlled morphology for nanopatterning is to develop ordered microphase-separated morphology by considering the time scale for segregation, namely segregation strength during solvent evaporation. The induced orientation is attributed to the permeation discrepancy between phase-separated microdomains. The perpendicular morphology is initiated from the air surface, and formed in order to create an optimized condition (i.e. the fastest path) for solvent evaporation whereas parallel morphology may impede the evaporation of solvent molecules. Following the nucleation of microphase separation, the perpendicular morphology can be kinetically induced by solvent evaporation.

Keywords: Spin coating; Solution casting; Degradable block copolymer

1. Introduction

Recently, a variety of new patterning technologies have been developed, which try to create nanometer scale periodic patterns over large areas. Different methods for nanopatterning such as photolithography, soft lithography, scanning probe lithography, electron lithography (i.e. top-down methods) and self-assembly of living cells, surfactants, dendrimers and block copolymers (i.e. bottom-up methods) have been proposed and examined [1]. Among them, self-assembled block copolymers driven by the immiscibility between the constituted blocks possess inherently rich morphologies such as lamellae, cylinders, spheres and gyroids [2]. In contrast to the lithographic methods, the formation of nanopatterns from the self-assembly of block copolymers can be efficiently, economically achieved due to the ease of processing. For such nanopatterns to prove useful in applications, it is necessary to generate thin-film samples with well-oriented periodic arrays over large area. Different approaches to control over the orientation of phase-separated microdomains have been achieved by using solution casting [3–9], shear fields [10–14], electric fields [15,16], surface effect [17–19], patterned substrates [20–22], temperature gradients [23], graphoepitaxy [24,25] and epitaxial crystallization [26–28]. To fulfill the prerequisites of practical applications, the methods for orientation control are required to generate uniform, thin

* Corresponding author. Address: Department of Chemical Engineering, National Tsing-Hua University, Hsinchu 30013, Taiwan, ROC. Tel.: +886 3 5738349; fax: +886 3 5715408.
E-mail address: rmho@mx.nthu.edu.tw (R.-M. Ho).

0032-3861/$ - see front matter © 2005 Elsevier Ltd. All rights reserved.
doi:10.1016/j.polymer.2005.07.069

enough films with oriented microdomains. Furthermore, the controlled thin films are expected being able to form onto different substrates. Hexagonal cylinder (HC) morphology is the most used microstructure for nanopatterning. Recently, a very rapid route to generate oriented HC microdomains by spin coating for poly(styrene)-*b*-poly(-ethyleneoxide) (PS–PEO) has been reported; within seconds, arrays of mesoscopic cylindrical microdomains of PEO were produced in a glassy PS matrix to open a novel route towards water permeable membranes with well-defined channel size [29]. In addition to the control of microdomain orientation, lateral ordering of the mesoscopic domains can also be achieved by solvent annealing [30].

Block copolymers containing aliphatic polyesters draw extensive attention in the preparation of mesoporous polymers attributed to the ease degradation of ester groups. The polyesters can be selectively degraded, particularly by hydrolysis [31]. Ordered mesoporous polymers from poly(styrene)-*b*-poly(D,L-lactide) (PS–PLA) block copolymers has been successfully achieved by hydrolysis of the PLA in the bulk [32]. In this study, a series of degradable block copolymers, poly(styrene)-*b*-poly(L-lactide) (PS–PLLA), with PLLA HC morphology has been synthesized. By selecting appropriate solvents for spin coating, the formation of large-size, oriented microdomains of PS–PLLA thin films where the axis of HC morphology is perpendicular to the substrate (i.e. perpendicular morphology) was successfully achieved. Nanopatterned thin films with uniform surface and controlled thickness can be simply obtained by spin coating onto different substrates. Nanopatterned templates can thus be prepared after hydrolysis. Systematical studies with respect to the formation of perpendicular morphology were carried out to examine the possible origins for the induced orientation. As observed, the formed morphology by spin coating was strongly dependent upon the use of solvents attributed to the effect of solvent evaporation rate and solvent miscibility between constituted blocks. Selective and neutral solvents with different evaporation rates were thus used to examine the true origins for the formation of perpendicular morphology. The present studies relate generally to an efficient way for producing large-scale, well-oriented nanochannel arrays in the form of thin films by using degradable block copolymers.

2. Experimental

2.1. Materials

A series of PS–PLLA copolymers with PLLA volume fraction ranging from 0.25 to 0.35 were prepared by using two-step polymerization sequence. Free radical polymerization of styrene using 4-hydroxy-2,2,6,6-tetramethylpiperidine-*N*-oxyl, 4-Hydroxy-TEMPO (4-OH-TEMPO), as initiator in the presence of dibenzoylperoxide (BPO) resulted in a hydroxyl-terminated polystyrene. The PS-TEMPO-4-OH further reacts with $[(\mu_3\text{-EDBP})Li_2]_2$ $[(\mu_3\text{-}^n\text{Bu})Li(0.5Et_2O)]_2$ giving a macroinitiator. The $[(\mu_3\text{-EDBP})Li_2]_2$ $[(\mu_3\text{-}^n\text{Bu})Li(0.5Et_2O)]_2$ was prepared according to the method described previously [33]. Followed by the control ring-opening polymerization of L-lactide in the presence of the macroinitiator, PS–PLLA was then prepared. The detailed synthetic routes and conditions were reported in our previous paper [34].

The gel permeation chromatography (GPC) measurements were performed on a Hitachi L-7100 system equipped with a differential Bischoff 8120 RI detector using THF (HPLC grade) as an eluent. Molecular weight and molecular weight distributions were calculated using polystyrene as standard. The number average molecular weight (M_n) of 4-hydrolysis-TEMPO terminated PS and polydispersity (PDI) of PS–PLLA block copolymer were obtained by GPC analysis. The molecular weight of PLLA blocks was measured by ^{1}H NMR analysis. On the basis of molecular weight and volume ratio, these PS–PLLAs (Table 1) are designated as PS*x*–PLLA*y* ($f^v_{PLLA} = z$). *x* and *y* represent the numbers of repeating units for PS and PLLA blocks measured by NMR, respectively, and *z* indicates the volume fraction of PLLA calculated by assuming densities of PS and PLLA are 1.02 and 1.248 g/cm^3.

Table 1
Varieties of synthesized PS–PLLA block copolymers having HC microstructures

Entry	$M_{n,PS}$ (g/mol)	$M_{n,PLLA}$ (g/mol)	PDI	f^v_{PS}	*d*-Spacing (nm)			Diameter (nm)		
	[a]	[b]			[c]	[d]	[e]	[c]	[d]	[e]
PS83–PLLA41	8900	5900	1.15	0.65	12.7	16.8	20.8	7.2	12.2	10.1
PS198–PLLA71	20,700	10,200	1.17	0.71	25.8	28.4	32.9	13.8	18.9	19.7
PS280–PLLA97	29,400	14,000	1.21	0.72	31.4	37.2	35.5	16.7	23.5	20.0
PS365–PLLA109	38,200	15,700	1.21	0.75	34.1	39.7	44.2	17.0	24.6	20.9

[a], Measured from GPC analysis; [b], obtained from integration of ^{1}H NMR measurement; [c], obtained from calculation of TEM micrographs; [d], determined from first scattering peak of SAXS; [e], obtained from surface analysis of SPM.

The block copolymers of polystyrene-*b*-poly(D,L-lactide) (PS–PLA) were also prepared by using two-step polymerization sequence. The detailed synthetic routes were similar to the methods by Pan and co-workers [35], and briefly described below. A double-headed initiator, $HOCH_2$-$CH(CH_3)_2CH_2O$–C(=O)$CHCl(CH_3)$ (DHI4–Cl), was first prepared. Hydroxyl-terminated polystyrene (PS–OH), was then prepared by the bulk atom transfer radical polymerization (ATRP) of styrene with DHI4–Cl as an initiator and CuBr/HMTETA as the catalyst/ligand. The PS–PLA was synthesized using the PS–OH as macroinitiator, and $Sn(OCt)_2$ as catalyst. The M_n of the PS–PLA synthesized were determined by NMR analysis as 53,000 g/mol whereas the PDI was determined by GPC as 1.26. The volume fraction of PLA was calculated as 0.27 by assuming densities of PS and PLA are 1.02 and 1.18 g/cm^3.

2.2. Sample preparation

Bulk samples of block copolymers were prepared by solution casting from dichloromethane (CH_2Cl_2) solution (10 wt% of PS–PLLA or PS–PLA) at room temperature. Thin films of the block copolymer were first formed on different substrates by solution casting and spin coating from dilute solution (1.5 wt% of PS–PLLA) at room temperature. All the samples prepared by spin coating were carried out at spin rate of 1500 rpm unless specified. Small amount of PS–PLLA or PS–PLA solution (ca. 0.075 ml) was directly delivered onto target substrate on spin coater during spinning. Thin-film sample on target substrate was formed within seconds, and then the sample was observed by microscopes without further treatment.

2.3. Differential scanning calorimetry (DSC)

DSC experiments were carried out in a Perkin–Elmer DSC 7 for the measurements of thermal behavior of PS–PLLA and PS–PLA. For instance, PLLA blocks of PS365–PLLA109 ($f^{v}_{PLLA} = 0.25$) melt at around 157 °C. The glass transition temperatures of PLLA and PS are approximately 45 and 95 °C, respectively. Similar measurements have also been carried out for various PS–PLLA and PS–PLA samples synthesized in this study. It is interesting to observe that the crystallization rate is extremely low for the PLLA blocks in phase-separated PS–PLLA microdomains. No significant exothermic response was observed under fast cooling. The significant decrease in crystallization rate is attributed to the confinement effect for crystallization. By contrast to the crystallizable PS–PLLA, the PS–PLA samples were identified as non-crystallizable polymers.

2.4. X-ray experiments

Small-angle X-ray scattering (SAXS) experiments were conducted at the synchrotron X-ray beam-line X27C at the National Synchrotron Light Source in Brookhaven National Laboratory. The wavelength of the X-ray beam is 0.1366 nm. The zero pixel of the SAXS patter was calibrated using silver behenate, with the first-order scattering vector q^* ($q^* = 4\lambda^{-1}\sin\theta$, where 2θ is the scattering angle) being 1.076 nm^{-1}. Time-resolved SAXS experiments were carried out in a heating chamber with step temperature increasing. Degradation temperature was identified by the disappearance of scattering peaks.

A Siemens D5000 1.2 kW tube X-ray generator ($Cu\ K_\alpha$ radiation) with a diffractometer was used for wide-angle X-ray diffraction (WAXD) powder experiments. The scanning 2θ angle ranged between 5 and 40° with a step scanning of 0.05° for 3 s. The diffraction peak positions and widths observed from WAXD experiments were carefully calibrated with silicon crystals with known crystal size.

2.5. Transmission electron microscopy (TEM)

Thin sections of solution-cast PS–PLLA bulk samples having thickness about 50 nm were obtained by ultra-cryomicrotomy using a Reichert Ultracut microtome. Bright field TEM images were obtained by mass-thickness contrast on a JEOL TEM-1200× transmission electron microscopy, at an accelerating voltage of 120 kV. Staining was accomplished by exposure the samples to the vapor of a 4% aqueous RuO_4 solution for 2 h. Spin-coated PS–PLLA thin films on carbon-coated glass slides were directly examined by TEM. After staining, the thin films were stripped and floated onto the water surface and then recovered using copper grids. Bright field images of mass-thickness contrast were obtained from the stained samples. The ED experiments for the thin films were also carried out.

2.6. Scanning probe microscopy (SPM)

SPM images by tapping mode were obtained from thin-film samples. A Seiko SPA-400 AFM with a SEIKO SPI-3800N probe station was employed at room temperature in this work. A rectangle-shaped silicon tip was applied in dynamic force mode (DFM) experiments using a type of SI-DF20 with a spring force contact of 14 N m^{-1} and scan rates of 1 Hz. The thin-film thickness was determined by SPM. First, the thin-film samples were scratched by using sharp knife to create cutting edge for thickness measurements. The topographic profile of the scratched sample was then examined by SPM where the step depth of cutting edge was measured as sample thickness. For comparison, surface profiler (Dektak II A) was used to measure the sample thickness by simply scanning the sample surface from center to the edge of spin-coated samples. Also, the method for the thickness measurement by SPM described by Möller and co-workers was used [36]. Consistent results were obtained by using different methods.

2.7. Field-emission scanning electron microscopy (FESEM)

FESEM observations were performed on a JEOL JSM-6700F using accelerating voltages of 1.5 keV. Samples were examined either on the spin-coated surface or fractured cross section of PS–PLLA thin film after hydrolysis. The samples were mounted to brass shims using carbon adhesive, and then sputter-coated with 2–3 nm of platinum (the platinum coating thickness was estimated from a calculated deposition rate and experimental deposition time).

3. Results and discussion

3.1. Phase-separated morphology

The self-assembly morphology of PS–PLLA block copolymers in bulk state was studied by TEM and SAXS. As observed, crystallization of PLLA in PS–PLLA might give rise to significant changes for microphase-separated morphology of PS–PLLA. To relieve the disturbance of PLLA crystallization on formed morphology, cast samples

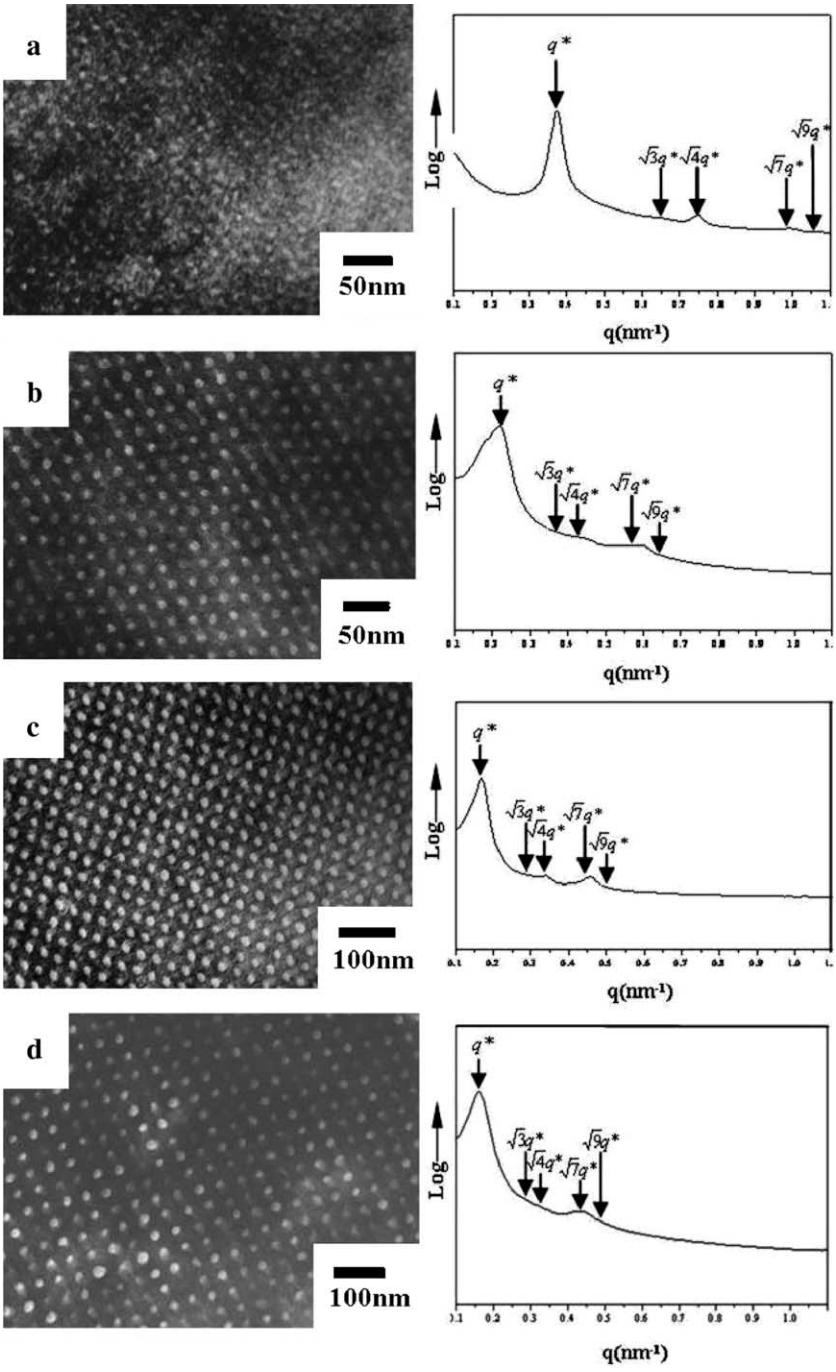

Fig. 1. The TEM micrographs of solution-cast (a) PS83–PLLA41 ($f_{PLLA}^{v} = 0.35$); (b) PS198–PLLA71 ($f_{PLLA}^{v} = 0.29$); (c) PS280–PLLA97 ($f_{PLLA}^{v} = 0.28$) and (d) PS365–PLLA109 ($f_{PLLA}^{v} = 0.25$). The corresponding azimuthally scanned one-dimensional SAXS profiles are also obtained as shown.

were annealed at temperature above PLLA melting but below order–disorder transition temperature, and then quenched in liquid nitrogen. The order–disorder transition temperature of PS–PLLA was above degradation temperature (~170 °C) as identified by SAXS. Amorphous PS–PLLA was obtained after the thermal treatments as evidenced by DSC and WAXD. DSC thermogram appeared no melting endotherm during heating. WAXD diffraction exhibited amorphous diffraction profile. After quench from microphase-separated melt, the thermally treated samples were then sectioned by ultra-microtome after RuO_4 staining. HC microstructures were identified by TEM and SAXS (Fig. 1). As observed by TEM, the microdomains of PS component appeared relatively dark after staining by RuO_4, while the microdomains of PLLA component appeared light. Corresponding SAXS results further confirmed the observed HC microstructure where the scattering peaks occurred at q^* ratio of $1:\sqrt{3}:\sqrt{4}:\sqrt{7}:\sqrt{9}$. These results are consistent with the hexagonally packed cylindrical microstructures. Similar results for the structure identification of various PS–PLLA samples having different molecular weight were also obtained. Consequently, various PS–PLLA samples having HC morphology were prepared (Table 1).

3.2. Induced orientation of PS–PLLA thin films

As described, the criteria for polymeric nanopatterns in applications are to generate well-oriented periodic arrays over large area, in addition to uniform surface with controlled thickness, in the form of thin films. To fulfill the requirements, one of the most convenient ways is to carry out nanopatterning directly by spin coating. It is well known that the formation of thin-film samples can be easily accomplished onto different substrates by spin coating. Thus, whether microphase-separated microstructure orients becomes the essential matter for nanopatterning by spin coating. Similar to the results of Russell and co-workers [29,30], large-size, oriented PS–PLLA microdomains can be simply obtained by spin coating where the axis of HC morphology is perpendicular to the substrate (i.e. perpendicular morphology) was obtained (Fig. 2(a)). As observed, the phase images of SPM observation under dynamic force mode exhibited approximately the top view of hexagonally packed cylindrical texture whereas dark PS matrix indicated less phase delay than bright PLLA dispersed domains. The perpendicular morphology was further examined by TEM as shown in Fig. 2(b) where the projected image reflects well-oriented perpendicular cylinders on the substrate. Moreover, no significant crystalline diffraction was identified as evidenced by selected area electron diffraction (SAED) experiments; suggesting that amorphous samples were obtained after spin coating. The oriented microdomains having perpendicular morphology can be as large as several cm^2 in area even though the hexagonal packing might not be perfectly arranged. As discussed by Lin and co-workers, the oriented effect for block copolymer microstructures is attributed to kinetic reasons for the formation of microphase-separated morphology during spinning [29]. Consequently, the spin-coated morphology is a non-equilibrium state.

3.3. Evaporation rate and solubility effects on orientation

Our results indicated that the induced orientation of microphase-separated morphology was strongly dependent upon different factors such as evaporation rate of solvent and its solubility between constituted blocks as well as spinning conditions (for instance, the temperature of coater, the concentration of solution and so on). It has been reported by Kim and co-workers that the selection of solvent for the casting of thin-film samples is critical to the final morphology of block copolymer microphase separation, particularly the orientation of microstructures [3]. Similarly,

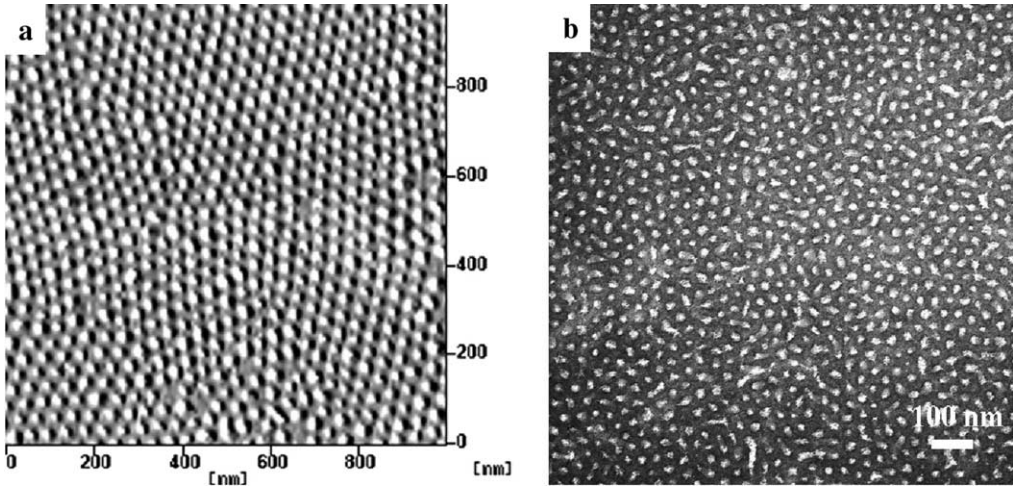

Fig. 2. (a) The tapping-mode SPM phase image and (b) TEM image stained by RuO_4 for spin-coated PS365–PLLA109 ($f^v_{PLLA} = 0.25$) thin films on glass slide from chlorobenzene.

well-defined perpendicular morphology can be obtained by spin coating using suitable solvents in this study. Systematic studies with respect to the controlling factors for induced orientation by spin coating were thus carried out in our lab.

The origins of the induced orientation are primarily attributed to the selection of appropriate solvent evaporation and its solubility between constituted blocks besides the processing conditions. Different solvents including PS selective and neutral solvents were used for comparison. To define the selectivity of solvents, the equation: $\chi = \chi_H + \chi_S = V_i(\delta_i - \delta_j)^2/RT + 0.34$ was used for nonpolar system, where V is the molar volume and δ is the solubility parameter for solvent i and polymer j [37]. The solubility parameter of PS and PLLA are 18.8 $(MPa)^{0.5}$ and 22.2 $(MPa)^{0.5}$, respectively [37,38]. The enthalpic component of polymer–solvent interaction parameter (χ_H) can be related to the solubility parameters via $\chi_H = V_i(\delta_i - \delta_j)^2/RT$. The entropic term ($\chi_S$) for nonpolar systems is usually taken to be a constant between 0.3 and 0.4 ($\chi_S = 0.34$ is often used). For a polymer to be soluble in a solvent at a particular temperature, χ must be below 0.5 even at high levels of polymer concentration in solution. On the basis of the above evaluation, chlorobenzene, benzene and THF were thus defined as PS selective solvent attributed to $\chi_{PS-solvent} < 0.5$ and $\chi_{PLLA-solvent} > 0.5$. By contrast, 1,2-dichloroethane (at which $\chi_{PS-solvent} < 0.5$ and $\chi_{PLLA-solvent} < 0.5$) is neutral solvent in this study. However, the 1,1,2-trichloroethane and chloroform are well-known good solvent for PLLA in experiments even though the $\chi_{PLLA-solvent}$ is above 0.5 [39]. The inconsistency probably results from the polar entities between polymer and solvent so that the χ should be smaller than the estimated value (i.e. $\chi_{PLLA-solvent}$ is below 0.5). As a result, 1,1,2-trichloroethane and chloroform are also referred as neutral solvent in this study. The details of selectivity and vapor pressure for solvents were listed in Table 2.

PS selective solvents having various vapor pressures at ambient temperature were used for spin coating to study the evaporation rate effect. As shown in Fig. 3, fast-evaporation conditions (for instance the use of THF solvent) generated a typical disorder microstructure (Fig. 3(a)) with evidence of microphase separation but poorly defined microdomains and no long-range order due to the limited time for the formation of microphase separation. The Fourier-transform result from the disordered texture exhibited diffuse scattering results as shown in the inset. Decreasing the evaporation rate tended to form fairly ordered morphology with slightly preferential orientation, as shown in Fig. 3(b). The formation of well-defined microstructure with perpendicular morphology was obtained by using suitable PS selective solvents, namely solvents with intermediate-evaporation rates. Fig. 3(c) shows the formed morphology at which PLLA cylinders are arranged in a hexagonal-like array within PS matrix as evidenced by the SPM phase image, and appears as perpendicular morphology after spin coating by using chlorobenzene (vapor pressures ~12 mmHg at ambient temperature). In contrast to the disordered morphology, the Fourier-transform pattern exhibits reflections with approximate six-fold symmetry. Further decreasing the evaporation rate may initiate morphological distortion and microdomain disorientation. To exaggerate the causes of low-evaporation rate effect on morphological distortion and controlled orientation, very slow evaporation-rate conditions were achieved by covering the coater with a jar for spin coating. As shown in Fig. 3(d), distorted, microphase-separated morphology with randomly oriented texture was obtained; suggesting that the perpendicular morphology will be interrupted by the slow-evaporation process. The Fourier-transform pattern thus appears scattering pattern with less diffusion. The causes of the interruption will be discussed below.

Neutral solvents have different vapor pressures at ambient temperature were also used for spin coating in order to examine the solubility effect on formed morphology. In contrast to the PS selective solvents, highly disordered microphase-separated morphology was obtained by spin coating using neutral solvents (Fig. 4). Even at suitable evaporation rates (for instance, the use of dichloroethane and trichloroethane solvents) as shown in Fig. 4(b) and (c), they still appear as disordered morphology after spin coating. To further confirm the disorder morphology of thin films from neutral solvent, the thin-film samples were examined by TEM. Consistently, typical disorder, microphase-separated morphology was identified in all thin film samples from neutral solvent (Fig. 5). As a result, the formation of perpendicular morphology of PS–PLLA thin films by spin coating strongly depends on the selection of solvents, particularly the corresponding solubility with constituted blocks.

Table 2
The selectivity and vapor pressure of solvents

Solvent	Molar volume (cm^3/mol)	$\chi_{PS-solvent}$	$\chi_{PLLA-solvent}$	$\delta_{solvent}$ $(MPa)^{0.5}$	Vapor pressure (mmHg)
Chlorobenzene	102.1	0.36	0.62	19.6	12
Benzene	89.4	0.34	0.81	18.6	70
THF	81.7	0.35	0.6	19.4	176
1,1,2-Trichloroethane	100.4	0.36	<0.5	19.6	17.1
1,2-Dichloroethane	79.2	0.42	0.44	20.4	61
Chloroform	80.7	0.34	<0.5	19	159.6

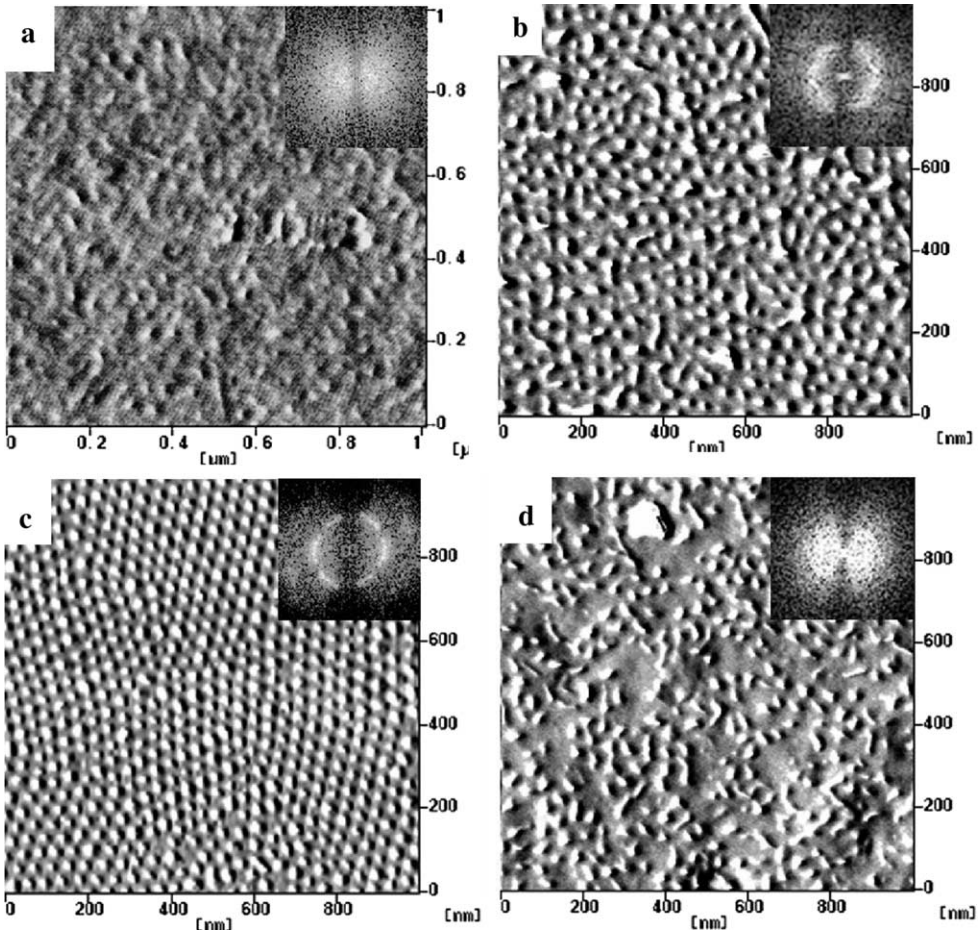

Fig. 3. The tapping-mode SPM phase images of the surfaces of spin-coated PS365–PLLA109 ($f^{v}_{PLLA} = 0.25$) thin films on glass slide by using different selective solvents for spin coating: (a) THF (vapor pressure at 20 °C: 131.5 mmHg); (b) benzene (vapor pressure at 20 °C: 70 mmHg); (c) chlorobenzene (vapor pressure at 20 °C: 12 mmHg); (d) very slow evaporation rate. The insets show the Fourier-transform patterns of the SPM images.

3.4. Molecular weight effect

Different PS–PLLA samples having various molecular weights were also used to study the molecular weight effect on formed morphology. The PS–PLLA thin-film samples with the molecular weights varying from 14,800 to 53,900 g/mol were prepared by spin coating using PS selective solvents with appropriate evaporation rates. The detailed molecular weight data of those samples were listed in Table 1. The effect of molecular weight is shown by Fig. 6. The SPM phase images of spin-coated thin films indicate that the formation of perpendicular morphology with

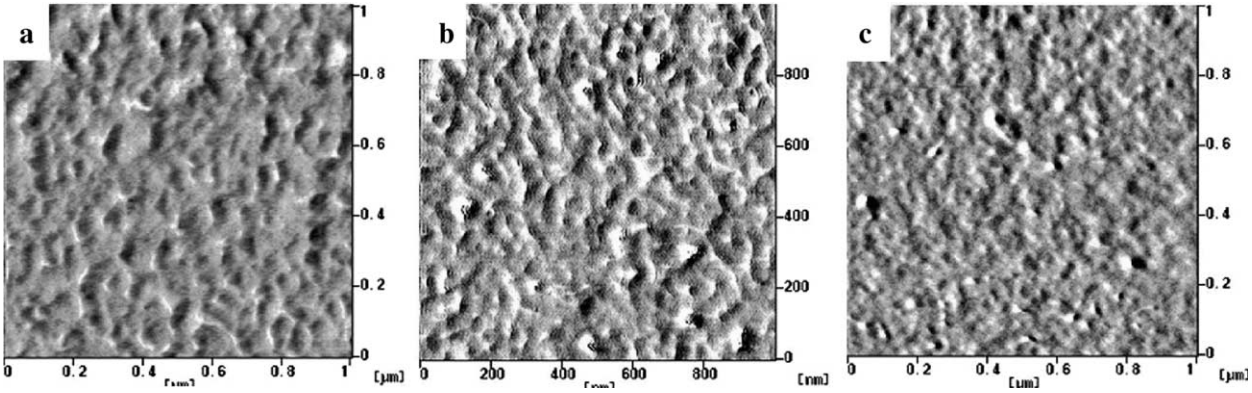

Fig. 4. The tapping-mode SPM phase images of the surfaces of spin-coated PS365–PLLA109 ($f^{v}_{PLLA} = 0.25$) thin films on glass slide by using different neutral solvents for spin coating: (a) Chloroform (vapor pressure at 20 °C: 159.6 mmHg); (b) 1,2-dichloroethane (vapor pressure at 20 °C: 61 mmHg); (c) 1,1,2-trichloroethane (vapor pressure at 20 °C: 17.1 mmHg).

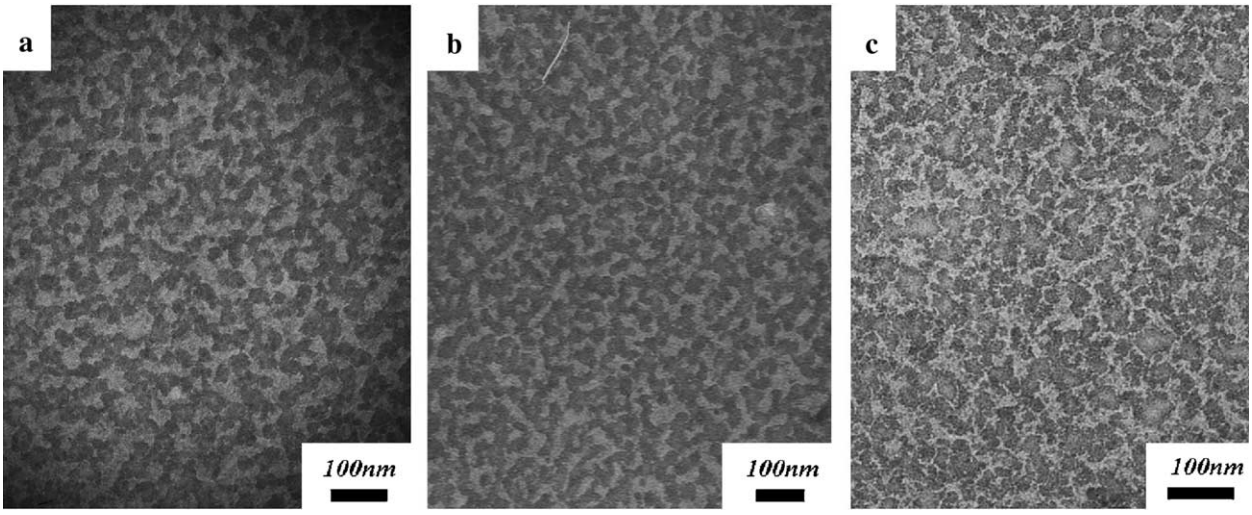

Fig. 5. The TEM images of the spin-coated PS365–PLLA109 ($f^{v}_{PLLA} = 0.25$) thin films on glass slide by using different neutral solvents for spin coating: (a) Chloroform (vapor pressure at 20 °C: 159.6 mmHg); (b) 1,2-dichloroethane (vapor pressure at 20 °C: 61 mmHg); (c) 1,1,2-trichloroethane (vapor pressure at 20 °C: 17.1 mmHg).

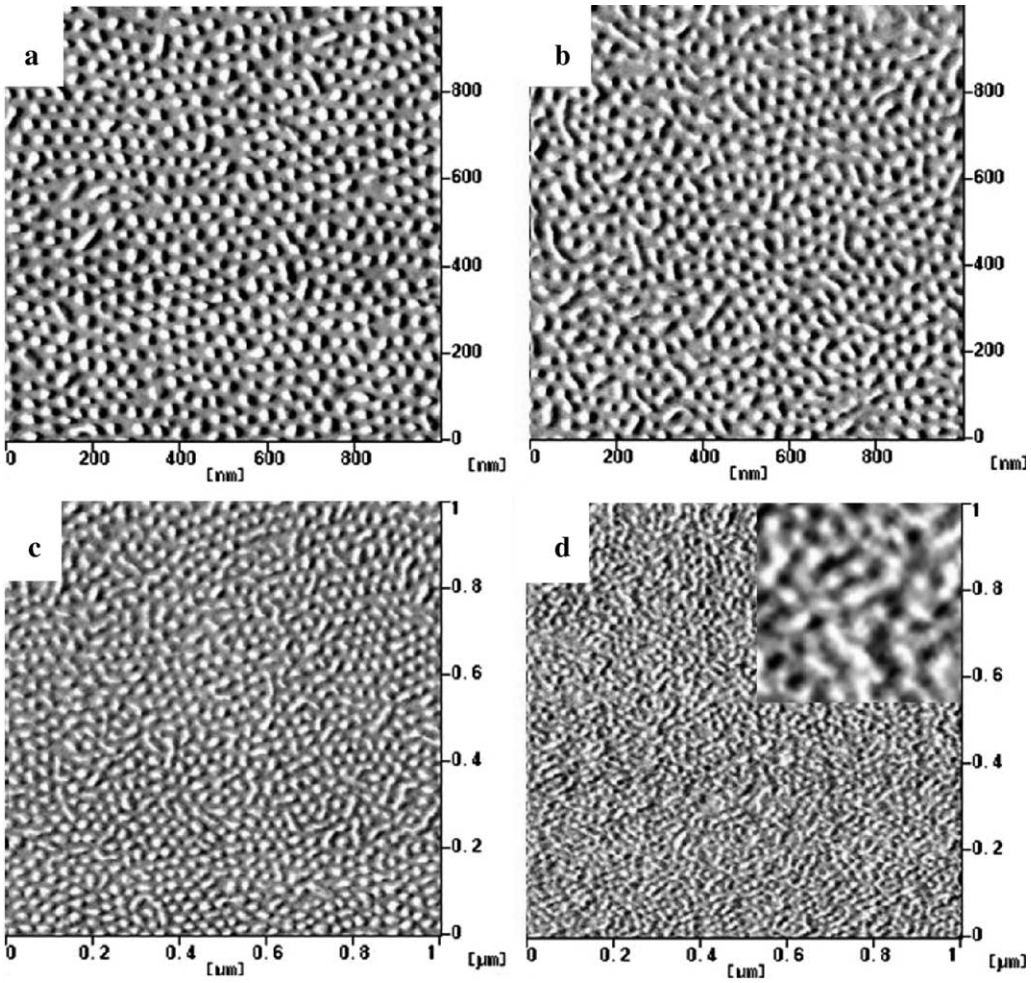

Fig. 6. The tapping-mode SPM phase images of spin-coated thin films on glass slide from chlorobenzene: (a) PS365–PLLA109 ($f^{v}_{PLLA} = 0.25$); (b) PS280–PLLA97 ($f^{v}_{PLLA} = 0.28$); (c) PS198–PLLA71 ($f^{v}_{PLLA} = 0.29$) and (d) PS83–PLLA41 ($f^{v}_{PLLA} = 0.35$). The inset shows the enlarged area of the image.

well-defined microstructure is certainly dependent upon the molecular weight of sample. At high molecular weights, the formed morphologies exhibited well-defined, perpendicular textures (Fig. 6(a)). With decreasing the molecular weight, the regions of disordered morphology were gradually increased (Fig. 6(b) and (c)). In the case of the lowest molecular weight sample studied (Fig. 6(d)), disordered microphase-separated morphology was identified as shown in the inset. As a result, the order and the orientation of microphase-separated morphology will be gradually lost upon decreasing the molecular weight of PS–PLLA. It is also noted that the high molecular weight samples may cause the reduction in molecular mobility so as to decrease the order of microphase-separated morphology. We speculate that disorder morphology may form for extremely high molecular weight samples.

3.5. Spin coating versus solution casting

One of the critical advantages to exploit spin coating process for the preparation of thin-film samples from solution is the ability to generate thin films with uniform surface and controlled thickness. For the induction of orientation in microphase-separated morphology, it will be interesting to compare spin coating process with solution casting. Fig. 7(a) shows the microphase-separated morphology of solution-cast samples from chlorobenzene (a PS selective solvent). In contrast to spin-coated samples (Fig. 3(c)), the SPM phase images of the solution-cast films exhibited typical spherulite-like morphology with evidence of branching crystalline lamellae; no ordered microphase-separated morphology can be observed. As a result, we suggest that the well-defined microphase-separated morphology from casting will be perturbed by the crystallization of PLLA during evaporation process, namely solvent-induced crystallization. The results are similar to the use of solvents with extremely low-evaporation rates at which solvent-induced crystallization effect starts playing important role on formed morphology. Considering the drawback of solvent-induced crystallization on microphase separation, non-crystallizable amorphous PS–PLA was used for nanopatterning. In contrast to the solution-cast samples of semi-crystalline PS–PLLA (Fig. 7(a)), well-defined microstructure with perpendicular morphology of PS–PLA thin films were observed through solution casting (Fig. 7(b)). These observations further confirm that solvent-induced crystallization is indeed critical to the formed morphology through casting.

As observed, the formed morphology is achieved by the choice of selective solvents. To examine the solubility effect on solution-cast morphology, neutral solvents having appropriate vapor pressures were also used for nanopatterning. Similar to the PS selective solvents, a spherulite-like morphology was obtained in PS–PLLA thin films by solution casting using neutral solvents (as shown in Fig. 8(a) for 1,1,2-trichloroethane solvent). So, the formation of spherulite-like texture is attributed to the solvent-induced crystallization regardless of the solubility concerns. In the case of amorphous PS–PLA, highly disordered morphology was obtained by using neutral solvents (as shown in Fig. 8(b) for 1,1,2-trichloroethane solvent). As a result, the formation of ordered, microphase-separated morphology cannot be achieved by solution casting using neutral solvents whether in PS–PLLA or PS–PLA thin films.

Since the perpendicular morphology can be obtained in PS–PLA thin films by solution casting using PS selective solvents, the next question is how the microphase-separated morphology of PS–PLA develops by spin coating. Fig. 9 shows that the spin-coated PS–PLA thin films from chlorobenzene appeared less-defined microphase-separated morphology where large-scale oriented morphology is absent. The discrepancies in the formed morphology in-between spin-coated and solution-cast PS–PLLA thin films will be discussed below.

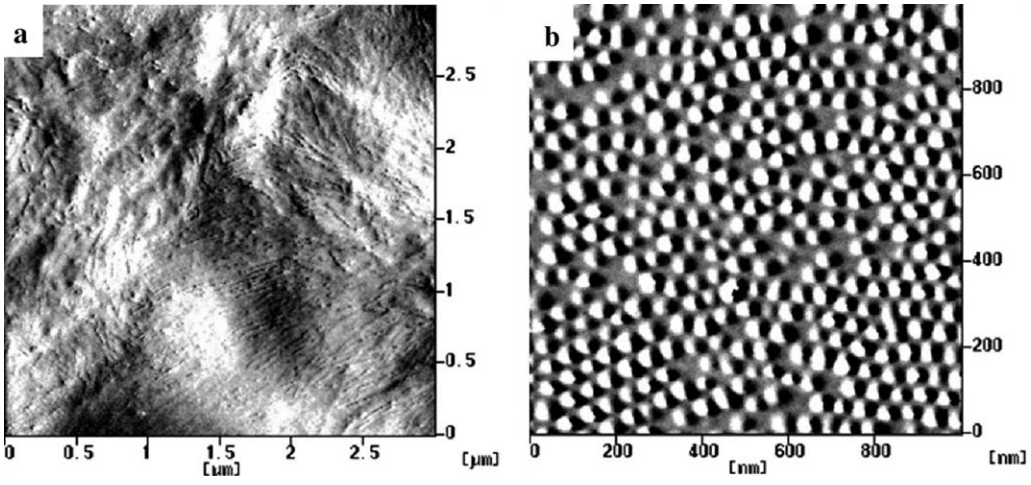

Fig. 7. The tapping-mode SPM phase images of solution-cast film on glass slide from selective solvent (chlorobenzene) at (a) PS365–PLLA109 ($f^{v}_{PLLA} = 0.25$) and (b) PS355–PLA112 ($f^{v}_{PLA} = 0.27$).

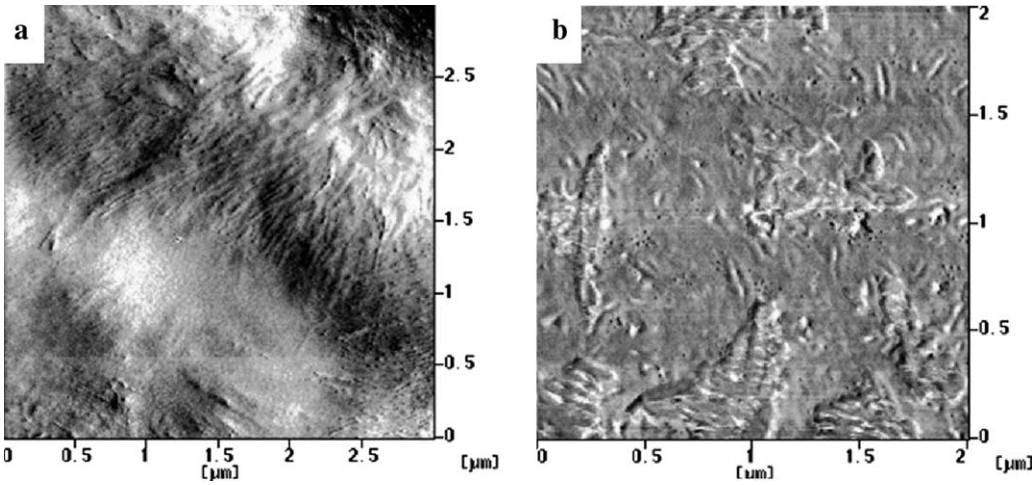

Fig. 8. The tapping-mode SPM phase images of solution-cast film on glass slide from neutral solvent (1,1,2-trichloroethane) at (a) PS365–PLLA109 ($f^{v}_{PLLA} = 0.25$) and (b) PS355–PLA112 ($f^{v}_{PLA} = 0.27$).

3.6. Substrate effect on oriented microdomains

For thin-film samples, it is inevitable to have influence, in particular the effects of affinity and surface tension, from the coated substrate. An interesting morphological evolution was observed at which the morphology at the bottom of formed nanopatterns on hydrophilic substrates appeared well-defined microstructure under SPM examination only if the film was treated by hydrolysis (i.e. degradation of PLLA; see below for details) (Fig. 10); suggesting that there is a thin layer of PLLA (for instance, ca. 5 nm as estimated by volume fraction for nanopatterning on glass slide having 50 nm film thickness) formed on the substrate after spin coating. To examine the substrate effect on formed thin-film morphology, the interfacial energy between homopolymer and substrate was determined by contact-angle measurements [40]. Films of PS ($M_w = 33{,}400$ g/mol) and PLLA ($M_w = 5020$ g/mol) with thicknesses of 20 nm were spin-coated directly onto the substrates. The samples were annealed in vacuum at 180 °C. After 24 h, the small homopolymer droplets could be observed on substrates by optical microscopy. Contact angles were measured on the droplets in de-wetted films by scanning probe microscopy at room temperature (below the T_gs of both homopolymer). According to the Young's equation, the interfacial energy between polymer and substrate could be estimated. The interfacial energy of PLLA–substrate system is qualitatively determined to be smaller than that of PS–substrate system in hydrophilic substrates (e.g. glass slide). It is noted that the surface tension of PS is comparable to that of PLLA [19]. We thus speculate that the preferential wetting of PLLA on hydrophilic substrates is mainly attributed to the significant affinity effect, namely the polar entity of PLLA. Interestingly, the formation of PLLA thin layer can be avoided by spin coating the samples at temperature above $T_{g,PLLA}$ (~45 °C) but below $T_{g,PS}$ (~95 °C) instead of at room temperature (Fig. 11). In contrast to Fig. 10, the bottom images appeared well-defined ordered microstructure as shown in Fig. 11(a) and (b) (height image and phase image, respectively) while spin coating was carried out at temperature above $T_{g,PLLA}$ but below $T_{g,PS}$ (e.g. 50 °C). The behavior has also been observed in different cases [3,5,29,30,41]; the glass transition temperature of at least one of the blocks should be below processing temperature in order to ease the substrate influence. This observation is in line with the suggested perpendicular morphology induced by spin coating. The thickness effect was also examined in this study. Various thicknesses of spin-coated thin films in a range from 30 to 200 nm were formed by controlling the rate for spin coating. Similar morphological results were observed in samples with different thicknesses. As a result, we speculate that the thickness effect is not an important control factor with regard to the formed morphology in this

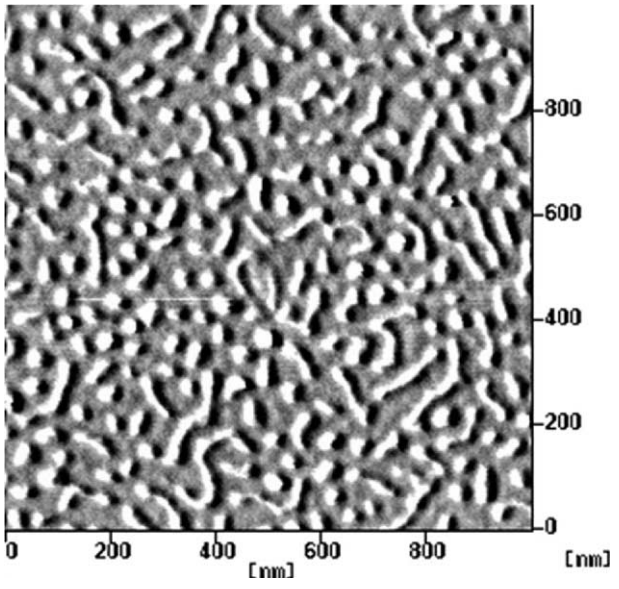

Fig. 9. The tapping-mode SPM phase images of spin-coated PS355–PLA112 ($f^{v}_{PLA} = 0.27$) thin films on glass slide from chlorobenzene.

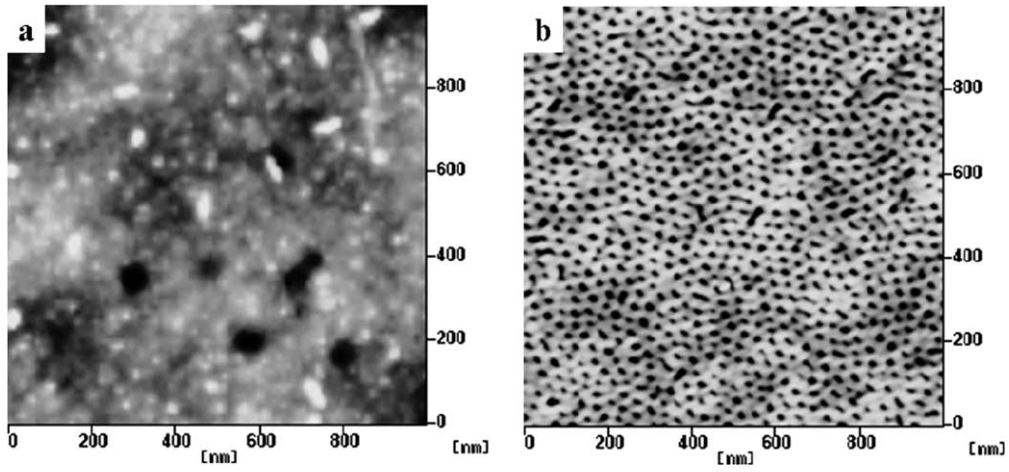

Fig. 10. (a) Before hydrolysis; (b) after hydrolysis of the tapping-mode SPM height images of the morphology at the bottom of nanopatterns for spin-coated PS365–PLLA109 ($f^{v}_{PLLA} = 0.25$) thin films on glass slide from chlorobenzene at ambient temperature.

thickness range studied. The origins of the formed morphology will be discussed below.

Considering the varieties of end use applications, different substrates including carbon-coated glass slide, glass slide, indium tin oxide (ITO) glass, silicon wafer, silicon oxide, inorganic light emitted diode and alumina have been used for nanopatterning. It is reasonable to infer that the formed morphology is affected by the selection of substrate. Usually, the thickness is the major factor to consider the significance of substrate effect. For thin films having thickness less than hundred nm as the examined samples here, it is inevitable to have influence from the coated substrate, particularly the effects of affinity and interfacial energy. These substrates used possess wide range of characteristics with respect to affinity and interfacial energy to PS–PLLA block copolymer. Nevertheless, similar morphological textures were obtained after spin coating regardless of the use of substrates. The morphologies on the top of nanopatterns formed on different substrates all exhibit perpendicular-like morphology (Fig. 12).

3.7. Origins of induced orientation

As observed, the formation of perpendicular morphology in microphase-separated block copolymer thin films from solution by solvent evaporation such as solution casting and spin coating is attributed to kinetic reasons. The phase transition from homogeneous solution state to microphase-separated morphology has been extensively studied in recent years [42–44]. The driving force of phase separation in block copolymer solution is, in principle, originated by the strength of segregation due to the incompatibility between constituted blocks. The segregation strength is usually referred to the value of χN, the product of incompatibility between the constituted block and the molecular weight of block copolymer. The formation of

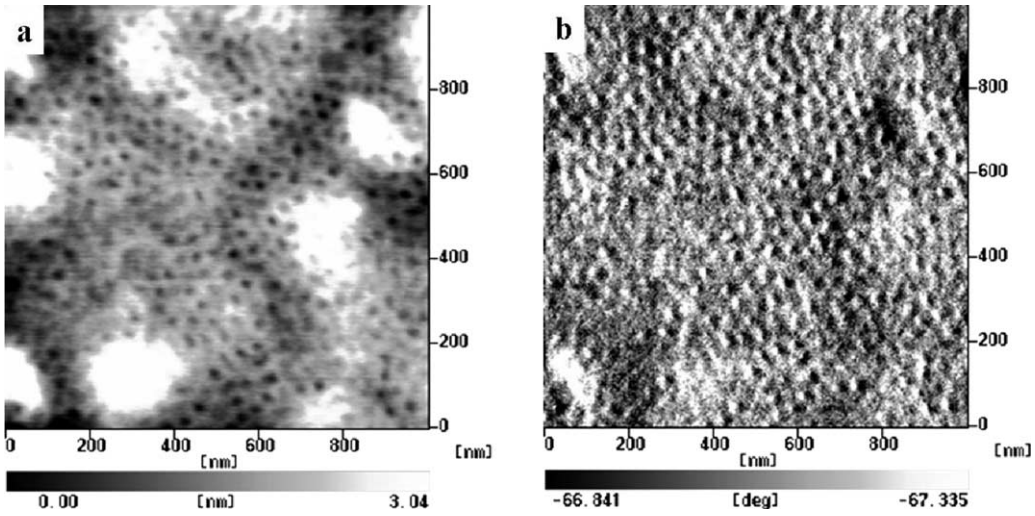

Fig. 11. The tapping-mode SPM (a) height and (b) phase image of the morphology at the bottom of nanopatterns for spin-coated PS365–PLLA109 ($f^{v}_{PLLA} = 0.25$) thin film on glass slide at 50 °C.

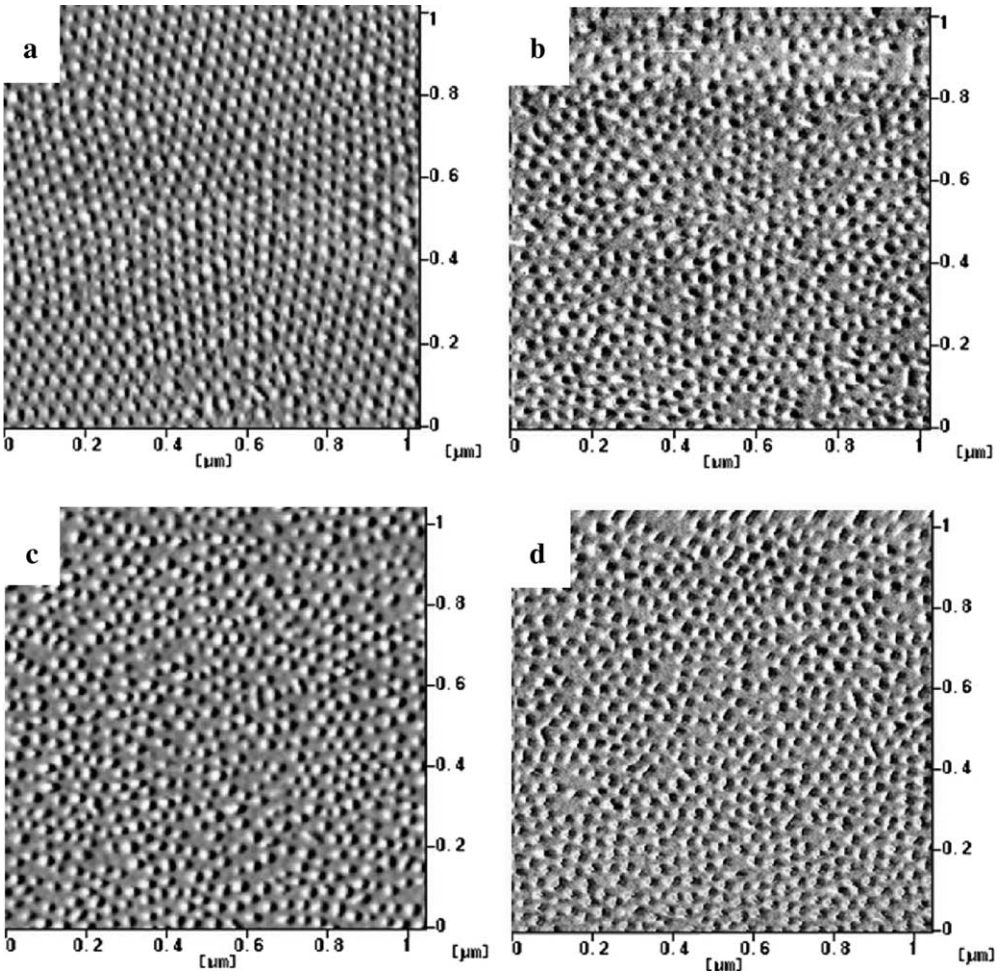

Fig. 12. The tapping-mode SPM phase images of spin-coated PS365–PLLA109 ($f^{v}_{PLLA} = 0.25$) thin films on various surfaces from chlorobenzene: (a) Glass slide; (b) carbon-coated glass slide; (c) indium tin oxide (ITO) glass; (d) silicon wafer.

final morphology is governed by the phase-transition processes (i.e. the kinetics of block copolymer self-assembly) during solvent evaporation, namely the elevation of sample concentration. We speculate that the segregation strength determines the time scale for the formation of microphase separation in this study. The higher the segregation strength is, the shorter the time required for microphase separation will be. The participation of solvent in the phase separation of block copolymers inevitably affects the segregation strength. Neutral solvent will decrease the segregation strength whereas selective solvent promotes the microphase separation. As a result, the use of neutral solvent requires longer time for the formation of well-developed microstructures. The ordered, microphase-separated morphology (Fig. 3(c)) was thus formed by spin coating for the use of selective solvents while strong enough segregation is available for the phase transformation. By contrast, poorly segregated, disordered morphology (Fig. 4) was obtained for the use neutral solvents due to insufficient time for the transformation. Owing to the fast process for film formation by spin coating, the evaporation process is too fast to achieve the defined microphase separation in neutral-solvent solution. Consequently, it is expected to form ordered morphology by using neutral solvents with lower evaporation rate. One of possible ways to slow the process is to carry out the solvent evaporation by solution casting using low-evaporation-rate neutral solvents. However, the slow process causes the solvent-induced crystallization of PLLA block upon solution casting so as to interrupt the formation of oriented morphology whether using the selective or neutral solvents (Figs. 7(a) and 8(a)). By contrast, perpendicular morphology can be successfully obtained by using non-crystallizable block copolymers, PS–PLA, through solution casting for selective solvents (Fig. 7(b)). Nevertheless, it is noted that the extremely slow process for solvent evaporation may lead to the formation of equilibrium morphology in thermodynamics. Namely, the substrate effect should be a significant factor to affect the final morphology. The orientation of microphase-separated microstructure is thus the results of thermodynamic and kinetic considerations (see below for detailed discussion). There exists an optimized condition for the formation of perpendicular morphology in PS–PLA thin films by solution casting. As a result, the segregation

strength upon solvent evaporation is the primary concern with respect to nanopatterning in order to form well-defined microphase-separated morphology. Similar justifications could also apply to the discrepancies in the formed morphology for different PS–PLLA samples having various molecular weights. As shown in Fig. 6, the order of microphase-separated morphology by spin coating is strongly dependent upon the molecular weight of PS–PLLA. The less defined microphase-separated morphology (Fig. 6(a)) is caused by the effect of low-molecular-weight PS–PLLA (i.e. the lower segregation strength) whereas distinct morphology is formed in high-molecular-weight samples (for instance Fig. 6(d)). Consistently, the formation of less defined morphology in spin-coated PS–PLA thin films as compared to that in PS–PLLA is also attributed to the segregation strength reasons. Our recent studies indicated that the incompatibility between PS and PLLA is obviously larger than that between PS and PLA [45]. Owing to the interaction parameter consideration, the lower segregation strength of PS–PLA samples is not able to form well-defined morphology by the fast evaporation process (i.e. spin coating) (Fig. 9). The interpretation can be further confirmed by the observation of disordered morphology (Fig. 8(b)) where the neutral solvents were used for solution casting. Although the evaporation rate is greatly decreased, the use of neutral solvent lowers the segregation strength of PS–PLA so as to cause the insufficient time scale for developing of microphase separation.

The next question will be how they form perpendicular morphology upon solvent evaporation. On the basis of thermodynamic considerations, the perpendicular morphology is in general slightly metastable relative to the parallel morphology [3]. As observed, the formation of PLLA perpendicular HC morphology without the formation of PLLA thin layer on coated substrate can only be obtained by spin coating the samples at temperature above $T_{g,PLLA}$ but below $T_{g,PS}$ (Fig. 13). We speculate that the perpendicular morphology is formed by well-controlled solvent permeation in block copolymers during solvent evaporation. It is well known that the permeation of solvent in polymer matrix is dependent upon its diffusivity in the matrix and its solubility with the polymer component. Considering the efficiency of solvent evaporation in block copolymers, it will be reasonable to expect that the solvent molecules preferentially go through the microphase-separated microdomains with higher permeation. As a result, the perpendicular morphology is formed in order to create an optimized condition (i.e. the fastest path) for solvent evaporation whereas parallel morphology may impede the evaporation of solvent molecules. Similar phenomena have been observed in different block copolymer systems and the behavior was discussed by different authors [3,5,29,30,41]. Usually, the diffusivities of small molecules in the rubbery and glassy states of polymeric materials are significantly different due to the free volume consideration. Dramatic increase in diffusivity from glassy to rubbery state can be recognized. In contrast to the significant effect on permeation due to the T_g consideration, the solubility also plays important role to determine the optimized diffusive path. So, the development of perpendicular morphology is attributed to the significant variation in permeation between PS and PLLA microdomains.

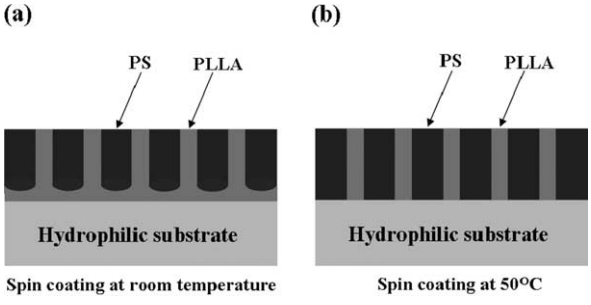

Fig. 13. The schematic illustration of cross-section view for PS–PLLA thin films by spin coating at (a) room temperature and (b) 50 °C.

The evolution of microphase separation is shown in Fig. 14. The microphase separation is initiated from the air surface at which the formed morphology adopts a perpendicular orientation due to permeation consideration, in particular the permeation of solvent to the surface. Following the nucleation of microphase separation, the solvent molecules are evaporated through the higher permeation microdomains so as to create solvent concentration gradient within the film. The development of perpendicular morphology continuously executes from the free surface due to the epitaxy-like growth through the entire film as described by Kim and co-workers [30]. The solvent-concentration gradient would be subtle under conditions where solvent is allowed to evaporate relatively fast. Eventually, the straight perpendicular HC morphology is formed from the top to the bottom in the direction of the maximum solvent-concentration gradient regardless of the characteristics of the used substrate. However, the development of perpendicular morphology may encounter significant change to equilibrium morphology (i.e. parallel morphology) due to the lower evaporation rate while the evolution of concentration gradient goes far from the free surface at which thermodynamic effect takes over to exert a determining influence on the morphology. Namely, thicker samples should be much obvious in according to the change of orientation. The substrate effect is now a predominated factor to affect the formed morphology. Consequently, parallel morphology might be formed due to the thermodynamic consideration. At ambient temperature for the thin-film formation of PS–PLLA, the PLLA block in PS–PLLA solution could run into glassy state during solidification so as to cause lower permeation for solvent evaporation. At near the interface of PS–PLLA thin film and substrate, the thermodynamic and substrate effects would define the orientation of microphase-separated microstructures due to the lower permeation. Thin-layer PLLA could be formed under conditions with low evaporation rate, particularly at

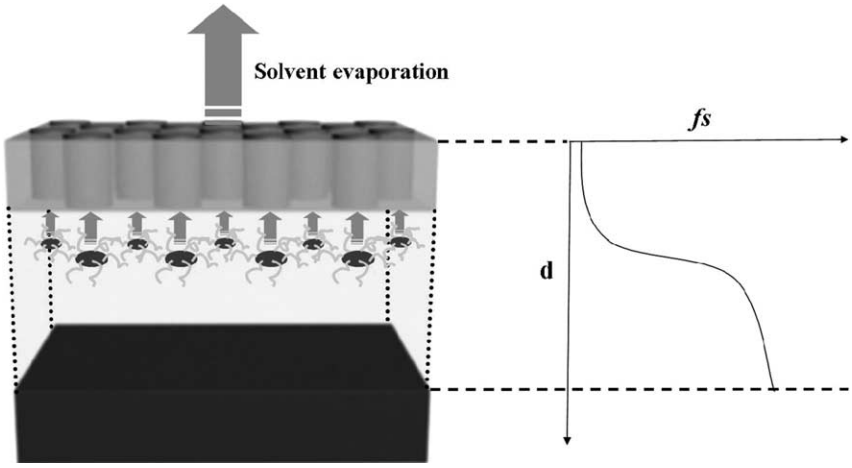

Fig. 14. The schematic illustration of formation of PS–PLLA nanopattern prepared by spin coating, similar to the mechanism proposed by Kim and co-workers, where f_s is the volume fraction of solvent and d is the depth of thin film [30].

hydrophilic substrates. By contrast, there is no PLLA thin layer while the casting is carried out at temperature above the glass transition of PLLA at which the evaporation rate should be fast enough to lead the kinetically controlled process.

As a result, the perpendicular HC morphology can be obtained by spin coating for the use of suitable solvents having appropriate evaporation rates at which well defined microphase-separated morphology should be able to develop by considering the time scale for segregation. Simultaneously, the perpendicular morphology is initiated due to the permeation discrepancy between microphase-separated microdomains so that fastest evaporation can be achieved. The metastable morphology is thus obtained.

3.8. Nanopatterned templates by hydrolysis

For practical applications, the constituted PLLA component might be selectively degraded by hydrolysis treatment to form regularly patterned topographic surface from the oriented microdomains of PS–PLLA thin-film samples. Following the successful procedure for hydrolysis of PLA described by Zalusky and co-workers [32], perpendicular HC nanochannel arrays as evidenced by FESEM observations (Fig. 15(a)) were simply obtained by using a sodium hydroxide solution of methanol/water. Moreover, the cylindrical nanochannels truly span the entire thickness of the films (Fig. 15(b)) in the hydrolyzed nanopatterns. Different domain sizes were obtained by controlling molecular weight of PS–PLLA. Consequently, nanopatterned templates over large area in addition to uniform surface with controlled thickness and domain size in the form of thin film were successfully prepared on different substrates as shown in Fig. 16. Here, we present an excellent and quick way to prepare large-scale microdomains for PS–PLLA diblock copolymers. Owing to the hydrolysis character of the polyester components, the formation of the perpendicular nanochannel arrays provides a simple path to prepare nanopatterned templates for applications.

One of the promising applications in nanopatterned templates is to carry out reaction within the ordered nanochannels (i.e. the concept of nanoreactor) so that periodic nanoarrays of materials, in particular for inorganic

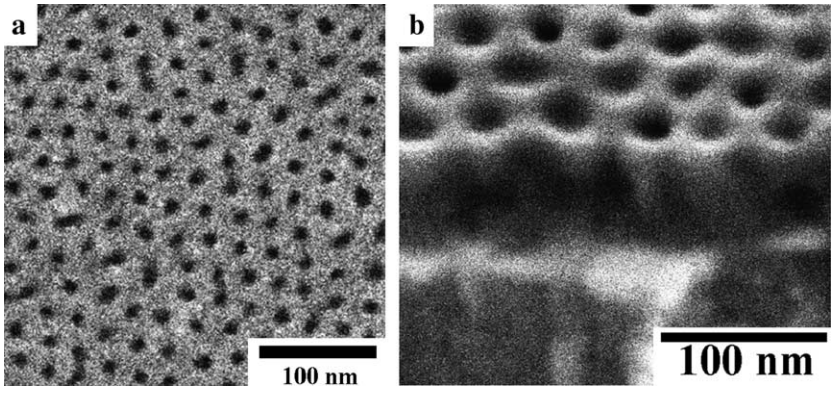

Fig. 15. The (a) top view and (b) cross-section view FESEM images of spin-coated PS365–PLLA109 ($f^{v}_{PLLA} = 0.25$) thin films on silicon wafer from chlorobenzene at 50 °C after hydrolysis.

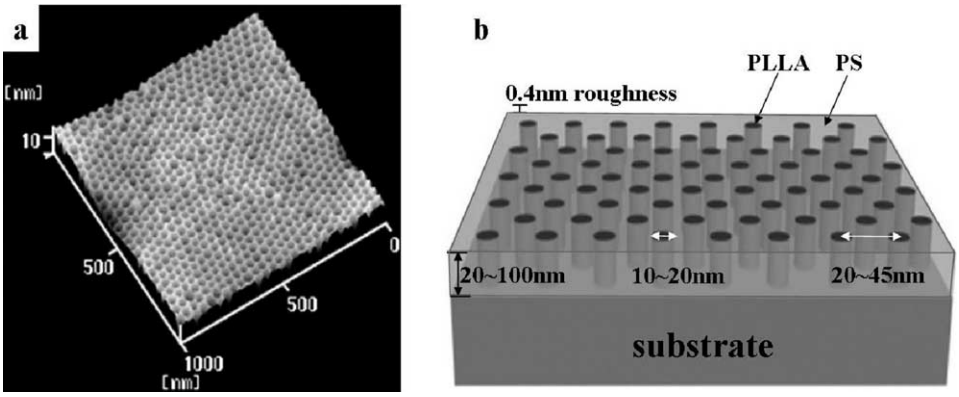

Fig. 16. (a) 3D tapping-mode SPM height image of SPM for spin-coated PS365–PLLA109 ($f^{v}_{PLLA} = 0.25$) thin films on glass slides after hydrolysis. (b) Schematic illustration of PS–PLLA nanopattern prepared by spin coating.

substances, can be efficiently created. Our recent results demonstrate the possibility to create inorganic nanoarrays (for instance, titania oxide) through the concept of nanoreactor. The cylindrical mesopores in the nanopatterns were served as the reactor to host the sol–gel reaction for the formation of titania oxide. Similar approaches can also be applied to a variety of inorganic materials.

4. Conclusion

Unique self-assembly morphology of the PS–PLLA thin films, large-size oriented microdomains with perpendicular morphology, was obtained. The formation of the nanopatterned microdomains is suggested to be in accordance with the effect of induced orientation by spin coating, regardless of the effects of film thickness and coated substrates. The mechanism of induced orientation for PS–PLLA microdomains is strongly dependent upon the evaporation rate of solvent and its solubility between constituted blocks. The perpendicular orientation of microdomains is attributed to the permeation discrepancy between phase-separated microdomains. Owing to the degradable character of the polyester component, the formation of the topographic nanopatterns of PS–PLLA by spin coating provides a simple path to prepare thin-film templates for the applications in nanotechnologies.

We thank Dr Benjamin S. Hsiao of Chemistry Department State University of New York at Stony Brook, Dr Shaofeng Ran and Dr Igors Sics of National Synchrotron Light Source at Brookhaven National Laboratory for their help in Synchrotron SAXS experiments. Our appreciation is extended to Ms P.-C. Chao and Mr Y.-F. Lu of Regional Instruments Center at NCHU and Ms S.-Y. Lee at NSYSU for their help in TEM, FESEM and WAXD experiments, respectively.

References

[1] For a recent review, see Park C, Yoon J, Thomas EL. Polymer 2003; 44:6725.
[2] Bates FS, Fredrickson GH. Annu Rev Phys Chem 1990;41:525.
[3] Kim G, Libera M. Macromolecules 1998;31:2569.
[4] Fukunaga K, Elbs H, Magerle R, Krausch G. Macromolecules 2000; 33:947.
[5] Temple K, Kulbaba K, Power-Billard KN, Manners I, Leach A, Xu T, et al. Adv Mater 2003;15:297.
[6] Van Dijk MA, Van den Berg R. Macromolecules 1995;28:6773.
[7] Mansky P, Harrison CK, Chaikin PM, Register RA, Yao N. Appl Phys Lett 1996;68:2586.
[8] Lammertink RGH, Hempenius MA, Van den Enk JE, Chan VZH, Thomas EL, Vancso GJ. Adv Mater 2000;12:98.
[9] Hahm J, Sibener SJ. Langmuir 2000;16:4766.
[10] Keller A, Pedemonte E, Willmouth FM. Nature 1970;225:538.
[11] Albalak RJ, Thomas EL. J Polym Sci, Part B: Polym Phys 1993;32:37.
[12] Koppi KA, Tirrell M, Bates FS. Phys Rev Lett 1993;70:1449.
[13] Chen ZR, Kornfield JA, Smith SD, Grothaus JT, Satkowski MM. Science 1997;277:1248.
[14] Albalak RJ, Thomas EL, Capel MS. Polymer 1997;38:3819.
[15] Morkved TL, Lu M, Urbas AM, Ehrichs EE, Jaeger HM, Mansky P, et al. Science 1996;273:931.
[16] Thurn-Albrecht T, Schotter J, Kästle GA, Emley N, Shibauchi T, Krusin-Elbaum L, et al. Science 2000;290:2126.
[17] Mansky P, Liu Y, Huang E, Russell TP, Hawker C. Science 1997;275: 1458.
[18] Huang E, Rockford L, Russell TP, Hawker CJ. Nature 1998;395:757.
[19] Olayo-Valles R, Lund MS, Leighton C, Hillmyer MA. J Mater Chem 2004;14:2729.
[20] Rockford L, Liu Y, Mansky P, Russell TP. Phys Rev Lett 1999;82: 2602.
[21] Heier J, Genzer J, Kramer EJ, Bates FS, Walheim S, Krausch GJ. Chem Phys 1999;111:11101.
[22] Kim SO, Solak HH, Stoykovich MP, Ferrier NJ, dePablo JJ, Nealey PF. Nature 2003;424:411.
[23] Hashimoto T, Bodycomb J, Funaki Y, Kimishima K. Macromolecules 1999;32:952.
[24] Segalman RA, Yokoyama H, Kramer EJ. Adv Mater 2001;13:1152.
[25] Cheng JY, Ross CA, Thomas EL, Smith HI, Vancso GJ. Appl Phys Lett 2002;81:3657.
[26] Wittmann JC, Lotz B. Prog Polym Sci 1990;15:909.
[27] De Rosa C, Park C, Thomas EL, Lotz B. Nature 2000;405:433.
[28] Ho RM, Hsieh PY, Tseng WH, Lin CC, Huang BH, Lotz B. Macromolecules 2003;36:9085.
[29] Lin Z, Kim DH, Wu X, Boosahda L, Stone D, LaRose L, et al. Adv Mater 2002;14:1373.
[30] Kim SH, Misner MJ, Xu T, Kimura M, Russell TP. Adv Mater 2004; 16:226.
[31] Tsuji H, Ikada Y. J Polym Sci, Part A: Polym Chem 1998;36:59.

[32] Zalusky AS, Olayo-Valles R, Taylor CJ, Hillmyer MA. J Am Chem Soc 2001;123:1519 [0.5 M solution was prepared by dissolving 2 g of sodium hydroxide in a 40/60 (by volume) solution of methanol/water at 60 °C for the degradation of amorphous PLLA].
[33] Ko BT, Lin CC. J Am Chem Soc 2001;123:7973.
[34] Ho RM, Chiang YW, Tsai CC, Lin CC, Ko BT, Huang BH. J Am Chem Soc 2004;126:2704.
[35] Tao L, Luan B, Pan CY. Polymer 2003;44:6725.
[36] Spatz JP, Sheiko S, Möller M. Adv Mater 1996;8:513.
[37] Mark JE. Physical properties of polymers handbook. New York: AIP Press; 1996.
[38] Blomqvista J, Mannforsa B, Pietilä LO. Polymer 2002;43:4571.
[39] Auras R, Harte B, Selke S. Macromol Biosci 2004;4:835.
[40] Vitt E, Shull KR. Macromolecules 1995;28:6349.
[41] Turturro A, Gattiglia E, Vacca P, Viola GT. Polymer 1995;36:3987.
[42] Hanley KJ, Lodge TP, Huang CI. Macromolecules 2000;33:5918.
[43] Lodge TP, Pudil B, Hanley KJ. Macromolecules 2002;35:4707.
[44] Lodge TP, Hanley KJ, Pudil B, Alahapperuma V. Macromolecules 2003;36:816.
[45] The order-disorder transition temperatures (T_{ODT}) of PS–PLLA and PS–PLA were measured by time-resolved SAXS experiments. With the evolution of the temperature, the discontinuity of the peak intensity of the first reflection peak occurred at 180 °C for PS37–PLLA42 ($f_{PLLA}^{v}=0.49$, $N=79$). By contrast, under the same degree of polymerization, the T_{ODT} of PS37–PLA42 ($f_{PLLA}^{v}=0.45$, $N=78$) as reported by Hillmyer and co-workers [46] was 116 °C. We thus speculate that the segregation strength of PS–PLLA is higher than that of PS–PLA due to the interaction parameter consideration.
[46] Zalusky AS, Olayo-Valles R, Wolf JH, Hillmyer MA. J Am Chem Soc 2002;124:12761.